

Iron silicides formation on Si (111)7x7 studied by scanning tunneling microscopy

ABDELBAKI CHEMAM^{a*}, MAHIEDDINE ALI RACHEDI^b

^a *Laboratoire d'Etudes des Surfaces et Interfaces de la Matière Solide –LESIMS, Université Badji Mokhtar Annaba, Algeria*

^b *Laboratoire d'Etudes et de Recherche des Etats Condensés-LEREC, Université Badji Mokhtar Annaba, Algeria*

The deposition of ferrocene [Fe (C₅H₅)₂] and iron pentacarbonyl [Fe (CO)₅] on Si(111)7x7 have been studied at room temperature. On Si(111)7x7, the adsorption sites have been identified by means of scanning tunneling microscopy. We propose a ferrocene adsorption model on Si(111)7x7, i.e., a di-sigma bridging by the molecule between an adatom and a restatom site similar to that proposed for the ethylene. For the iron pentacarbonyl, we have found evidence of a dissociative adsorption on nucleophilic sites. At a higher temperature, an exposure to iron pentacarbonyl lead to the growth of good quality iron silicide. Whereas, silicide carbide is formed on exposure to ferrocene. The films obtained can be explained by means of the chemisorption process at room temperature.

(Received April 17, 2013; accepted June 12, 2013)

Keywords: STM, Si (111)7x7, Adsorption, Iron pentacarbonyl, Ferrocene

1. Introduction

The chemisorption of the different molecules of the reacting gas at the substrate surface is the first stage of the layer growth by chemical vapor deposition. The chemisorption processes are then parameters which can influence the quality of the interfaces and layers. In this study, we were interested in the adsorption of ferrocene and iron pentacarbonyl on Si (111)7x7. Tunneling microscopy was used to identify the reactive sites of the Fe (CO)₅ and Fe(C₅H₅)₂ molecules on Si(111)7x7 surface. These metalorganic molecules have been used as gas vectors for silicide growth on silicon substrates. Iron silicide layers of good quality have been obtained with Fe(CO)₅ [5], whereas the use of Fe(C₅H₅)₂ leads to highly carbon contaminated films [6]. The aim of our article is to emphasize the relationship between the chemisorption of these molecules and the growth properties of the layer [1-4].

2. Substrates

2.1 Si (111) 7x7

The dimer adatom stacking-faulted DAS model proposed by Takayanagi and al.[7] is actually unanimously accepted for the Si (111) 7x7 reconstruction. This model is presented in Fig. 1, a cell covers a surface equivalent to 49 atoms of the (111) plane. A stacking fault is present in the first monoatomic layer, but it affects only half of the cell (on the left of Fig. 1). Therefore, the cell is divided into two parts; one is called the faulted part and the other the unfaulted part. It is at the antiphase lines demarcating these two parts that the atoms of the second layer form

dimers. Where these lines intersect, one of the second layer atoms is missing which leaves a place for a third layer atom. This is called the cornerhole. The cell contains 12 atoms placed so that each one of them saturates three atoms of the first layer. Six of the first layer atoms remain nevertheless unsaturated, we call them restatoms. Such a structure contains 19 dangling bonds, 12 arising from the adatoms, 6 from the restatoms and one from the cornerhole. There are 7 dangling bond types. Four issues from the adatoms: adatoms situated at the cell corner (corner adatom) or at the center of a cell side (center adatom) and located on the faulted or the unfaulted cell part. Two others issue from restatoms, one from the faulted part, and the other from the unfaulted. The last bond type comes from cornerholes. The density of states of these dangling bonds have been calculated [8] and also been measured [9] by scanning tunneling microscopy STM. In general, the density of filled states ascribed to the dangling bond is larger in the faulted part than in the unfaulted whereas there is not a notable difference between the two parts for the density of empty states. For the restatoms: only the presence of states situated about 0.5 eV under the Fermi level should be noted. The electronic properties of the cornerhole differ to those of the restatoms only by the presence of supplementary states about 0.1 eV under the Fermi level. For the adatoms: we notice the presence of empty and filled states situated respectively at 0.4 eV above and 0.3 eV under the Fermi level. It is generally accepted that the dangling bonds are the centers of chemisorption reactions. As the Si(111) Surface presents 7 types of such bonds, we expect different chemical behaviors. One way of quantifying the reactivity of a site is to look at its capacity to give or receive electrons under the influence of an external potential (created for example by an exterior atom).

Brommer and al. evaluate [8] this capacity by the local softness. The greater the density of the empty states (acceptor), or of filled states (donor), around the Fermi level, the greater the softness. The calculations of the softness on the dangling bonds of the Si (111) 7×7 give the following result [8]: For electrophilic reactants (absolute electronegativity greater than that of silicon), the sites most apt to give electrons are, in decreasing order, the cornerhole, the restatoms and the adatoms. The sites situated on the faulted cell part have a greater softness than those situated on the unfaulted one. For nucleophilic reactants (absolute electronegativity inferior to that of silicon), the sites most apt to receive electrons are, in decreasing order, the adatoms, the cornerhole and the restatoms.

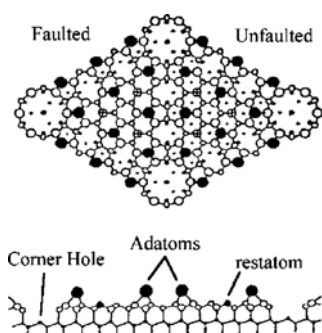


Fig. 1. Dimer adatoms stacking-faulted model of Si(111)7x7.

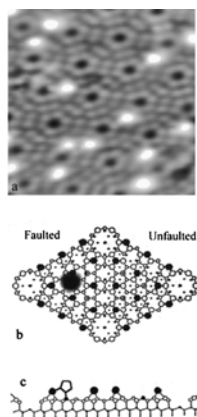


Fig. 2. (a) STM image (11 nm^2) of Si(111)7x7 surface exposed to 2L of ferrocene at ambient temperature. $V_{\text{sample}} = 13 \text{ V}$, $I = 170 \text{ pA}$. (b) Localization on DAS model of the large part of the protuberances created by adsorption. (Between a restatom and a center adatom, on faulted part). (c) Adsorption ferrocene on Si(111)7x7.

3. Adsorption of Fe (C₅H₅)₂ and Fe (CO)₅

3.1 Experimental methods

The experiments are carried out in an ultrahigh vacuum chamber (base pressure= 2×10^{-10} Torr) equipped

with an Auger electron analyzer and a scanning tunneling microscope working at room temperature. The tips used in STM are electrochemically fabricated from 0.25 mm diameter tungsten wire and cleaned in situ by electron bombardment heating. The samples are cut from doped Si(111) $\pm 0.25^\circ$ wafers; as doped wafers ($0.1 \Omega \text{ cm}$) are used for the preparation of Si(111)7×7 samples. The Si(111)7×7 surfaces are classically prepared by successive temperature flashes up to 1450 K followed by a cooling at 50 K/mn.

The reactive gases are introduced into the chamber through a leak valve. The gases are obtained from ferrocene, $[\text{Fe}(\text{C}_5\text{H}_5)_2]$, $P_{\text{sat}} = 8 \times 10^{-3}$ Torr or iron pentacarbonyl, $[\text{Fe}(\text{CO})_5]$, $P_{\text{sat}} = 35$ Torr vapors at room temperature. The exposure of the surface to the reactive gases is carried out one hour after the substrates preparation. We estimate, thereafter, that the sample temperature is lower than 350 K. The pressure of the gas introduced into the chamber is in the order of 10^{-7} Torr.

3.2 Adsorption of Fe(C₅H₅)₂ on Si(111)7x7

Fig. 2(a) shows a Si(111)7×7 surface after an exposure to 2 L of ferrocene. Modifications at the surface are clearly visible. White bumps appear mainly on the faulted half cells of the DAS structure, the bumps being situated in majority around the center adatoms. Their height is about 2 Å above the 7×7 adatoms. We have calculated the sticking coefficient of the ferrocene on the Si(111)7×7 to be about 5×10^{-2} . A statistical analysis of our images shows that the faulted half cell is five times more affected than the unfaulted one. The ratio of the number of white bumps situated around the center adatoms to that of those situated around the corner adatoms is 5. We notice that the majority of the white bumps on the Si(111)7×7 cell are located as shown in Fig. 2(b). The analysis by Auger electron spectroscopy (AES) of these samples shows that the ratio of the number of carbon atoms to that of iron is about 10. As only one single type of substrate modification is seen in STM images, this suggests that the adsorption leaves the Fe complex intact, a di-sigma bridging similar to that produced by the adsorption of the ethylene on Si(111)7×7 [10].

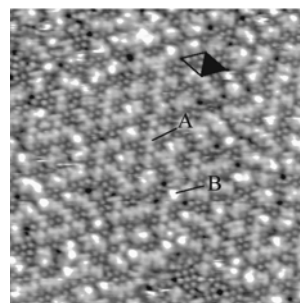


Fig. 3. STM image (34 nm^2) of a Si (111)7x7 surface exposed to iron pentacarbonyl. $V_{\text{sample}} = 12.3 \text{ V}$, $I = 55 \text{ pA}$. A 7×7 cell is drawn and the blackened part corresponds to the faulted part of the DAS structure.

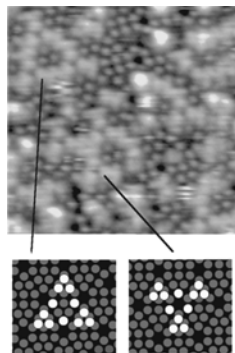


Fig. 4. Characteristic structures formed by $\text{Fe}(\text{CO})_5$ adsorption on $\text{Si}(111)7\times 7$ (15 nm^2). Grey ring: $\text{Si}(111)7\times 7$ adatoms, White ring: adsorption sites.

3.3 Adsorption of $\text{Fe}(\text{CO})_5$ on $\text{Si}(111)7\times 7$

Fig. 3 shows a $\text{Si}(111)7\times 7$ surface after an exposure to a few Langmuir of $\text{Fe}(\text{CO})_5$. Two types of modifications appear. The first type corresponds to white bumps mainly on the faulted part (1.5 \AA above the adatoms, Fig. 3 arrow B). The second corresponds to smaller bumps (0.5 \AA above the adatoms) which produce alignments parallel to the dimmers rows of the DAS structure (Fig.3. arrow A). The particular configurations of these base patterns form the characteristic structures that we observe on our image Fig. 4.

4. $\text{Fe}(\text{C}_5\text{H}_5)_2$ and $\text{Fe}(\text{CO})_5$ on $\text{Si}(111)7\times 7$ at a high temperature

The substrates are heated at temperatures from 700 to 900K and subjected to doses of 60 to 200 L of a reactive gas. Fig. 5 presents a $\text{Si}(111)7\times 7$ surface after an exposure to 200 L of ferrocene at 800 K and an annealing around 950K. Pyramidal triangular shaped aggregates are formed.

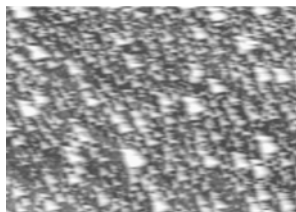


Fig. 5. STM image of a $\text{Si}(111)7\times 7$ surface exposed to 200 L of ferrocene at 800 K and annealed around 950 K. (600 nm^2).

Fig. 6 shows a $\text{Si}(111)7\times 7$ surface which has been exposed to 20 L of $\text{Fe}(\text{CO})_5$ at 800 K. Triangular shaped islands have grown. A 2×2 reconstruction on the islands is observed Fig. 7. Holes formed in the substrate are clearly visible at the edges of the aggregates situated on the terraces.

We notice that the density of the clusters is greater along the steps and the antiphase lines of the 7×7 domains than on the terraces. The clusters heights are multiples of 1.6 \AA with a predominance of even multiples. These results are comparable with other STM studies of iron silicides growth on $\text{Si}(111)7\times 7$ by solid phase epitaxy. The 2×2 reconstruction is characteristic of iron silicides [11].

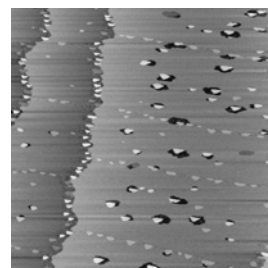


Fig. 6. STM image of a $\text{Si}(111)7\times 7$ surface exposed to 20 L of iron pentacarbonyl at 800 K.

5. Conclusion

In this paper, we have presented a study of room temperature chemisorption on $\text{Si}(111)$ of two organometallics (ferrocene and iron pentacarbonyl). The identification of the adsorption sites as well as the information obtained by Auger spectroscopy have allowed us to propose models of chemisorption for the two organometallic molecules. On the $\text{Si}(111)7\times 7$ surface, we propose a nondissociative adsorption for the ferrocene, i.e., a di-sigma bridging by the molecule between an adatom and a restatom site similar to that proposed for the ethylene. For the iron pentacarbonyl, we found evidence of a dissociative adsorption on nucleophilic sites. At a high temperature, an exposure to iron pentacarbonyl lead to the growth of good quality iron silicide. Whereas, silicide carbide is formed on exposure to ferrocene. The films obtained by GSRDE can be explained by means of the chemisorption process at room temperature.

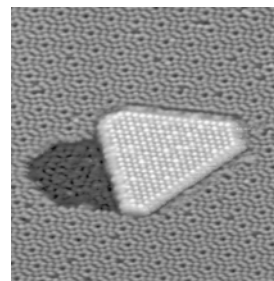


Fig. 7. Atomic resolution STM image on iron silicide island. $V_{\text{sample}} = -2.3\text{ V}$, $I = 35\text{ pA}$.

References

- [1] A. Wawro, S.Soto, R. Czajka et al, *Nanotechnology*, **19**(20), (2008).
- [2] Hara, Shinsuke, Yoshimura, Masamichi, Ueda, Kazuyuki, *Japanese Journal of Applied Physics*, **48**(8), (2009).
- [3] M. Krause, F. Blobner, L. Hammer et al, *Physical Review B*, **68**(12), (2003).
- [4] W. Weiss, M. Kutschera, Starke et al, *Surface Science*, **377**(1-3), 861 (1997).
- [5] G. J. M Dormans, *J. Cryst. Growth* **108**, 806 (1991).
- [6] H. Ch. Schfer, B. Rosen, H. Moritz, A. Rizzi, B. Lengeler, H. Luth, D. Gerthsen, *Appl. Phys. Lett.* **62**, 2271 (1993).
- [7] K. Takayanagi, Y. Tanishiro, S. Takahashi, M. Takahashi, *Surf. Sci.* **164**, 367 (1985).
- [8] K. D. Brommer, M. Galvan, A. Dal Pino, Jr., J. D. Joannopoulos, *Surf. Sci.* **314**, 57 (1994).
- [9] R. J. Hamers, R. M. Tromp, J. E. Demuth, *Phys. Rev. Lett.* **56**, 1972 (1986).
- [10] N. M. Piancastelli, N. Motta, A. Sgarlata, A. Balzarotti, M. De Crescenzi, *Phys. Rev. B* **48**(17), 892 (1993).
- [11] A. L. Vasquez de Parga, J. de la Figuera, C. Ocal, R. Miranda, *Europhys. Lett.* **18**, 595 (1992).

*Corresponding author: a.chemam@epst-annaba.dz